

LETTER • OPEN ACCESS

Influence of global warming on the rapid intensification of western North Pacific tropical cyclones

To cite this article: Nam-Young Kang and James B Elsner 2019 *Environ. Res. Lett.* **14** 044027

View the [article online](#) for updates and enhancements.

Environmental Research Letters



LETTER

Influence of global warming on the rapid intensification of western North Pacific tropical cyclones

OPEN ACCESS

RECEIVED

2 November 2018

REVISED

26 January 2019

ACCEPTED FOR PUBLICATION

28 February 2019

PUBLISHED

12 April 2019

Nam-Young Kang¹  and James B Elsner²¹ National Typhoon Center, Korea Meteorological Administration, Seoul 070762, Republic of Korea² Department of Geography, Florida State University, Tallahassee, FL 32306, United States of AmericaE-mail: nkang.fsu@gmail.com**Keywords:** tropical cyclone, western North Pacific, rapid intensification, global warming, efficiency of intensify

Original content from this work may be used under the terms of the [Creative Commons Attribution 3.0 licence](https://creativecommons.org/licenses/by/4.0/).

Any further distribution of this work must maintain attribution to the author(s) and the title of the work, journal citation and DOI.

**Abstract**

The rapid intensification (RI) of tropical cyclones (TCs) associated with global warming is a matter of concern worldwide. This study examines how the RI across the western North Pacific is related to the so-called ‘efficiency of intensify’ (EINT) environment induced by global warming. The EINT condition has been characterized by a strong anomalous high over an unstable tropical atmosphere, which supports efficient intensification. Here, we show that global warming significantly increases the proportion of RI-experiencing TCs through EINT environment. Global warming explains up to 51.3% of the variation in the proportion of RI-experiencing TCs with 93.0% of that related to EINT. Even the influence of El Niño and Southern Oscillation on the proportion of RI events, though small (16.1%), is mostly through an EINT environment (73.9%). Despite the increasing proportion of RI events among TCs, the number shows no trend over time as the EINT condition inhibits the number of overall TC occurrences. The findings are confirmed by the observational consensus between US Joint Typhoon Warning Center and Japan Meteorological Agency.

1. Introduction

Tropical cyclones (TCs) pose a chronic threat to personal life and property as well as to national socio-economic activities (Mendelsohn *et al* 2012, Houser *et al* 2014). As the concern about climatic change and global warming grows, rapidly intensifying TCs have become a serious focus for people around the globe. Anxiety is particularly widespread across the western North Pacific storm basin (100°E–180°) where there are more than fourteen countries and where more than one-third of all TCs worldwide occur (Kang and Elsner 2015). Super Typhoon Haiyan in 2013, with 6300 deaths and economic damages of the Philippines (NDRRMC 2014), is a particularly devastating example of just how quickly a intense TC can threaten and destroy inhabitants and their livelihood in vulnerable parts of this region.

TC intensity change results from a combination of many physical processes (Kowch and Emanuel 2015). Studies on TC intensity change and rapid intensification (RI) can be classified into three groups such as large-scale atmospheric, oceanic, and TC inner-core

processes (Gao *et al* 2016), which include vertical wind shear, upper-level tropospheric divergence, relative humidity, sea surface temperature, ocean heat content, eyewall replacement, and so on. Characteristics and mechanisms associated with RI have been explored mostly from an operational perspective (Wang and Zhou 2008, Rappaport *et al* 2012, Elsberry 2014, Emanuel 2017, Wang *et al* 2017). However, real-time forecasting of TC RI remains a big challenge as the myriad physical mechanisms and their environmental connections need greater clarification (Elsberry *et al* 2007, Kaplan *et al* 2010, Lin *et al* 2013, Rogers *et al* 2013).

Proximal factors influencing RI likely have colli-nearity since they are constrained by larger scale environmental variability (climate variables). A statistical model may show that a particular explanatory variable has a direct relationship (positive sign on the regression coefficient) with RI as the response variable but an indirect relationship (negative sign on the coefficient) with RI when more explanatory variables are included in the model. To make progress, here we focus on the connection of TC climate to the large-scale

environmental variability and then examine a possible link to TC RI.

From a climatological perspective, ‘efficiency of intensity’ (EINT) was suggested by Kang and Elsner (2012a). EINT indicates the gap between increasing intensity and decreasing frequency of annual TCs. EINT implies a large-scale environment with favorable conditions for the efficient intensification of TCs at the expense of overall occurrences. In follow-up studies, western North Pacific TC intensity metered by the annual mean of lifetime-maximum intensity (LMI) was interpreted as the influence of the synthetic environments constrained by the state of ENSO and superimposed by global ocean warmth (Kang and Elsner 2015, Yang *et al* 2018). Here, the synthetic environments means the combination of overall environmental factors at an indicated variability direction. They found that warming ocean significantly influences on the increasing EINT. In this study, the environmental connections to western North Pacific TC RI on an annual basis, are investigated especially focusing on global warming and EINT. Other factors such as ENSO and arrival time (AT) to LMI are also reviewed and compared to confirm the results.

Data used in this study are described in section 2. Subsequently, how to achieve observational consensus is addressed in section 3. Section 4 examines the trend of RI events, followed by the environmental review for the RI response in section 5. A summary is presented in section 6. All the analyses and figures are created using the software R (<https://r-project.org>) and are available from (<https://rpubs.com/Namyoungh/P2018c>).

2. Data

The Southern oscillation index (SOI) from the National Oceanic and Atmospheric Administration (NOAA)/Climate Prediction Center (<http://cpc.ncep.noaa.gov/data/indices/soi>) is used to indicate the state of ENSO. Extended reconstructed sea surface temperature version 4 (Huang *et al* 2015) and of the NOAA/National Centers for Environmental Prediction (NCEP) reanalysis (<http://esrl.noaa.gov/psd/data/gridded>) is used to calculate global mean sea surface temperature (GMSST) for identifying global ocean warmth. Geopotential height, air temperature, and specific humidity from NCEP reanalysis are also used for moist static energy (MSE). This study examines western North Pacific TC climate in best-track data from the US Joint Typhoon Warning Center (http://usno.navy.mil/NOOC/nmfc-ph/RSS/jtww/best_tracks) and from the Japan Meteorological Agency (<http://jma.go.jp/jma/jma-eng/jma-center/rsmc-hp-pub-eg/trackarchives.html>) as well. All statistics are for annual values of the variables averaged over the consecutive months of June through

November (JJASON) for the 30-year period of 1986–2015. The unit of TC winds is knot (kt) as recorded in the best-track data sets and as used by forecasters operationally.

3. Observational consensus

3.1. Inconsistency between best-track data sets

Special attention is paid to the different time periods for averaging maximum-sustained winds between the operational agencies. JTWC uses 1 min, while JMA uses 10 min for speed observations. Because of this difference the JTWC LMI span a larger range of values compared with the JMA LMI values, the differences of which can confound TC climate research studies (Kang and Elsner 2012b). As a way around this inconsistency, conversion rates for individual TC events have been sought (Knapp and Kruk 2010, Song *et al* 2010). However a quantile approach was recently suggested to compare the two sets of observations for climate studies (Kang and Elsner 2012b). The approach revealed remarkable similarity with LMIs from the two data sources matching at the same probability level after 1984, which is the year when the JMA began applying the Dvorak satellite analysis technique (Velden *et al* 2006) in operations (see www.wmo.int/pages/prog/www/tcp/documents/JMAoperationalTCanalysis.pdf). Chu *et al* (2002) addressed that JTWC intensities before 1985 also need to be used with care. Then, the beginning year of the current analysis is set as 1986 for a reliable consensus between different observations. On the basis of this quantile-matching finding, here an LMI conversion is used to match LMI quantiles between JTWC and JMA (table 1). Then the JMA LMIs are converted to new LMIs that are equivalent to the JTWC magnitudes. Now we have two data sets of 1 min LMIs that are subsequently used here.

3.2. Observational consensus on LMI distribution

Figures 1(a), (b) show the two-dimensional density distribution of LMI and its AT. The AT is the time difference between when the TC first reaches 34 kt and LMI in units of hours. Both observations of the same intensity scale (1 min average) referenced by JTWC magnitude, show a similar bimodal pattern. The peaks at higher intensity appear at almost the same location in both data sets. Overall, LMI increases with increases in AT (the density contours are aligned from lower left toward upper right), which can be understood as a TC needs sufficient time to mature. LMIs around the highest peak have larger spread indicating more variation than weaker LMIs.

Most studies define RI as the TC intensity change when 1 min average of maximum-sustained wind increases by at least 30 kt in 24 h (Kaplan and DeMaria 2003, Wang and Zhou 2008, Wang *et al* 2017). Here, the LMI events that experienced RI are selected according to this criteria and their density

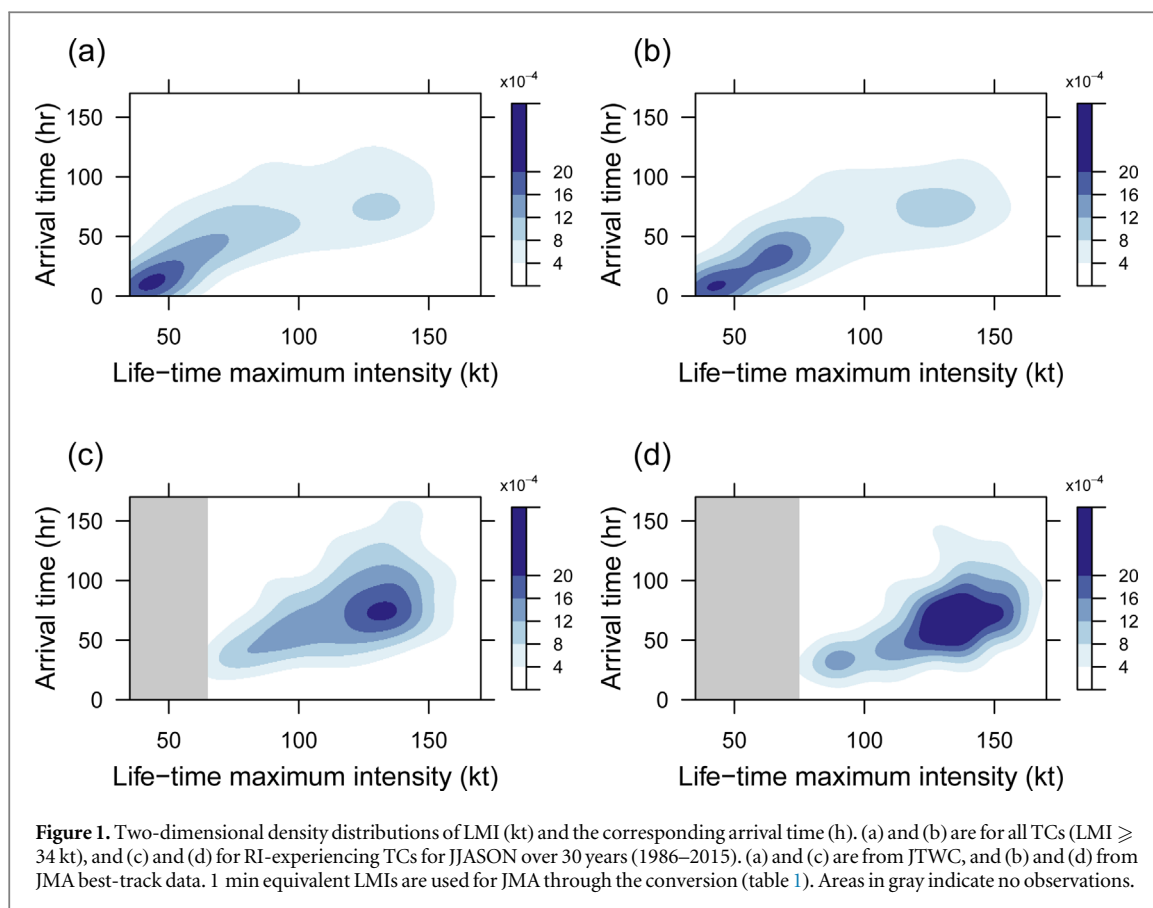


Figure 1. Two-dimensional density distributions of LMI (kt) and the corresponding arrival time (h). (a) and (b) are for all TCs ($LMI \geq 34$ kt), and (c) and (d) for RI-experiencing TCs for JJASON over 30 years (1986–2015). (a) and (c) are from JTWC, and (b) and (d) from JMA best-track data. 1 min equivalent LMIs are used for JMA through the conversion (table 1). Areas in gray indicate no observations.

Table 1. Conversion table for LMIs. LMIs come from JMA and JTWC best-track data sets, recorded at 5 kt intervals. JMA and JTWC use 10 min and 1 min wind averaging periods, respectively. 1 min equivalent JTWC LMIs refer to the values at the same probability level of JTWC LMIs from interpolated quantiles. Values are for the consecutive months of JJASON over the 30 year period of 1986–2015.

JMA LMI (kt)	Probability level (%)	1 min equivalent JTWC LMIs (kt)
35	6.6	35
40	14.6	42
45	23.7	48
50	32.4	55
55	39.3	64
60	43.9	71
65	48.7	75
70	54.7	86
75	61.5	92
80	68.7	106
85	75.2	116
90	80.1	124
95	85.4	129
100	92.4	138
105	95.2	140
110	98.3	152
115	99.4	156
120	99.7	158
125	100.0	170

distributions displayed in figures 1(c), (d). Allowing for different density levels, it is confirmed that the stronger peaks of LMI distributions can be attributed to RI-experiencing LMIs (Lee *et al* 2016). This study

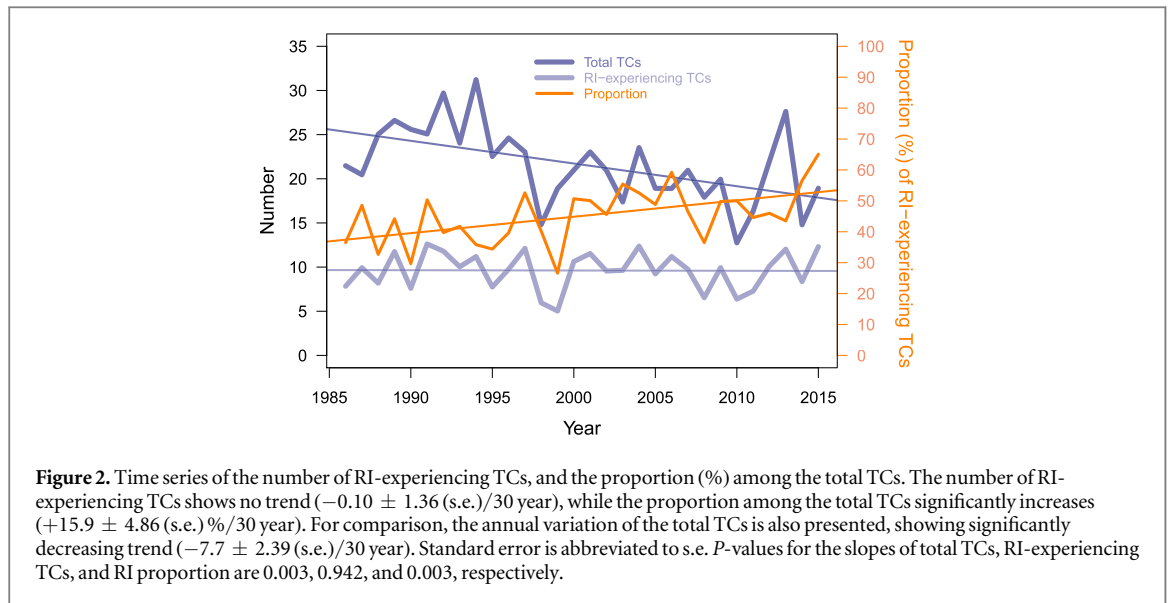
focuses on the RI-experiencing LMIs and their response to environmental conditions.

3.3. Merged TC climate indicators

For the present study, TCs are defined by cases with LMI exceeding 34 kt. First, annual values for TC frequency, intensity, proportion of RI-experiencing LMIs (Rip), and ATs over the period of 1986–2015 (using the consecutive months of June–November–JJASON) are determined from each 1 min best-track data set. Frequency is the total number of annual TCs with LMI exceeding 34 kt. Intensity is the annual average over all LMIs. Rip is the annual proportion of all TCs that experience RI. AT is the annual average ATs (h). Next, a merged set of the TC climate variations is formulated by the in-phase mode of the principal components using the two observation sources (JTWC and JMA) (Kang and Elsner 2016). Here, in-phase mode simply means the composition of the values having the same sign. Finally, the merged version of frequency, intensity, RI proportion, and AT is produced by standardizing the variation using the mean and variance of the JTWC observations.

4. Temporal variation of RI proportion

The annual (JJASON) number of TC occurrences shows a decreasing trend over the 30 years (1986–2015) with an average slightly more than 25 TCs at the start of the period dropping to less than 20



TCs at the end of the period. In contrast, the number of RI-experiencing TCs shows no trend with an overall average of about 10 TCs throughout the period (figure 2). Thus, the proportion of TCs undergoing RI has increased significantly over time. The RI-experiencing LMIs at the highest intensity level (see figure 1) suggest that increasing RI_p induces the strongest TCs getting stronger, which was also seen by the quantile method a decade ago (Elsner *et al* 2008).

The present TC intensification is understood as the representation of continuously warming influence on TC climate. Global ocean warmth indicated by GMSST is a useful environmental factor which directly estimates the warmth forcing on TC climate. Indeed, GMSST is strongly correlated with the magnitude of the trade-off between TC intensity and TC frequency (Kang and Elsner 2015). The trade-off implies the efficient intensification of TCs under the inhibition of occurrences, which is noted as the EINT (Kang and Elsner 2016, Yang *et al* 2018). EINT is calculated as

$$\text{EINT} = \left(\frac{\text{INT} - \mu_{\text{INT}}}{\sigma_{\text{INT}}} - \frac{\text{FRQ} - \mu_{\text{FRQ}}}{\sigma_{\text{FRQ}}} \right) / \sqrt{2}, \quad (1)$$

which is one of the principal components between TC intensity (INT) and frequency (FRQ), showing their out-of-phase relationship. Mean and standard deviation are denoted by μ and σ . INT and FRQ are vectors of annual values. EINT can be used as an indicator of the environment which intensifies TCs at the expense of the occurrences. Here we quantify how much of RI_p (percentage wise) is explained by GMSST and EINT and what environmental conditions are closely aligned with the explanatory variables.

5. Environmental review for the RI response

First, the variance partitions among RI_p, GMSST, and EINT are examined (figure 3(a)). Uncertainties are presented in table 2. As noted above, EINT is calculated as the out-of-phase mode of the principal components involving TC intensity and frequency. The area under the diagrammed arc within the circle, representing an environmental or TC variable, is the proportion of variance explaining annual variations in RI_p. Climatology shows that RI_p fluctuations are closely related to variations of EINT explaining 63.8% of the variability. Then, 51.3% of the variation in RI_p can be explained by GMSST, and the GMSST influence is mostly explained (93.0%) by EINT. In other words, nearly half of the increasing RI_p can be attributed to the EINT environment caused by global warming.

In addition, the ENSO influence on RI_p is evaluated (figure 3(b)). For this, negative SOI is used as the indicator of El Niño conditions. As expected, El Niño is seen to have an influence on RI_p, but only accounts for 16.1% of the variation. Though it explains only a small portion of RI_p variation, it is interesting that 73.9% of the El Niño influence is related to the EINT environment. Overall, EINT is identified as a dominant environment condition for RI_p, and thus a connector to global warming.

For additional support and as an aid to further understand the EINT environment as related to RI_p, next we consider the AT gap (AT_g) between the RI-experiencing LMIs and the annual total. That is, we express AT_g as

$$\text{AT}_g = \frac{\text{AT} - \text{AT}_{\text{RI}}}{\text{AT}}, \quad (2)$$

where AT denotes a vector of annual mean ATs (from 34 kt to LMI) over all TCs and AT_{RI} denotes a vector of annual mean RI-experiencing ATs. Since AT_{RI} contributes negatively in the formula, the value of AT_g

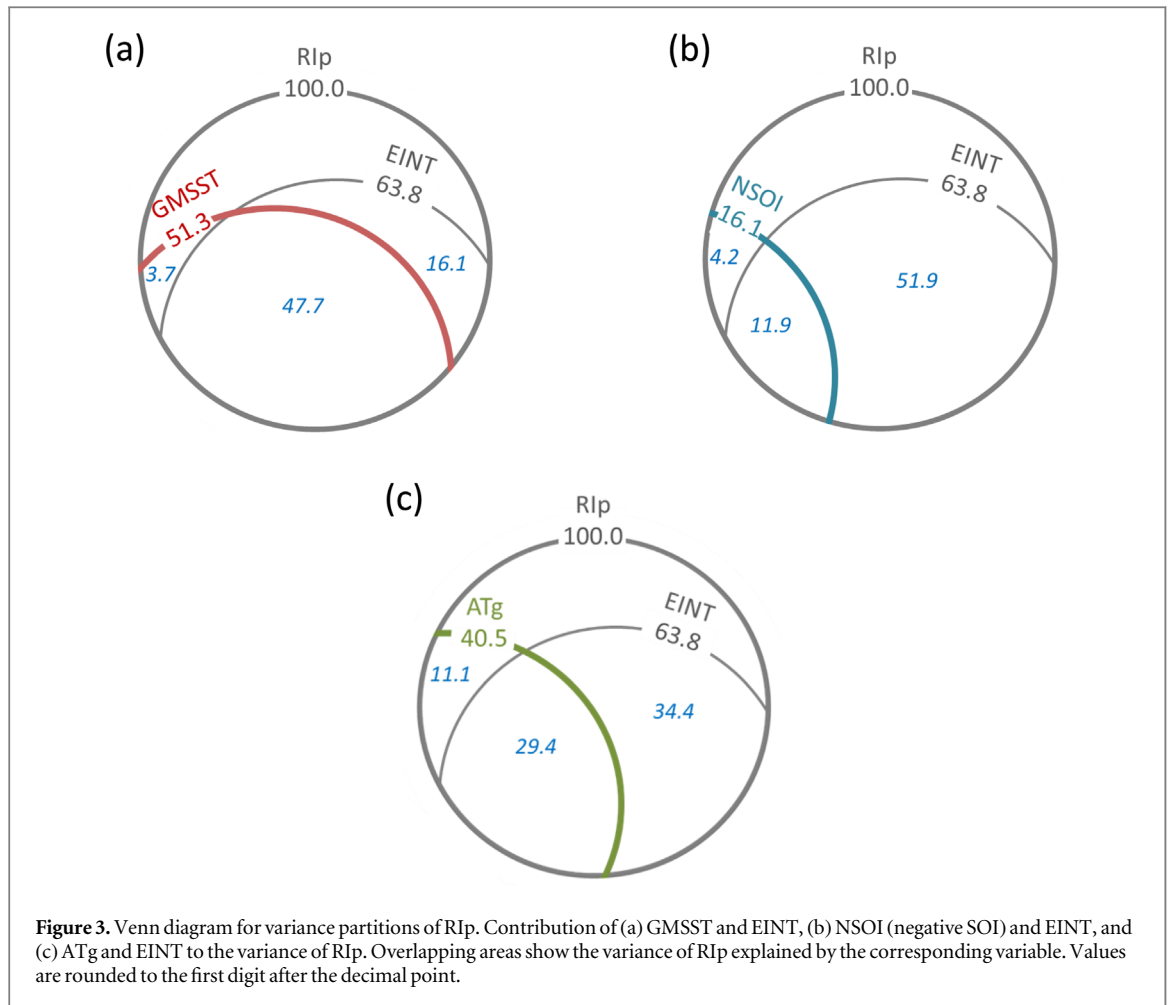


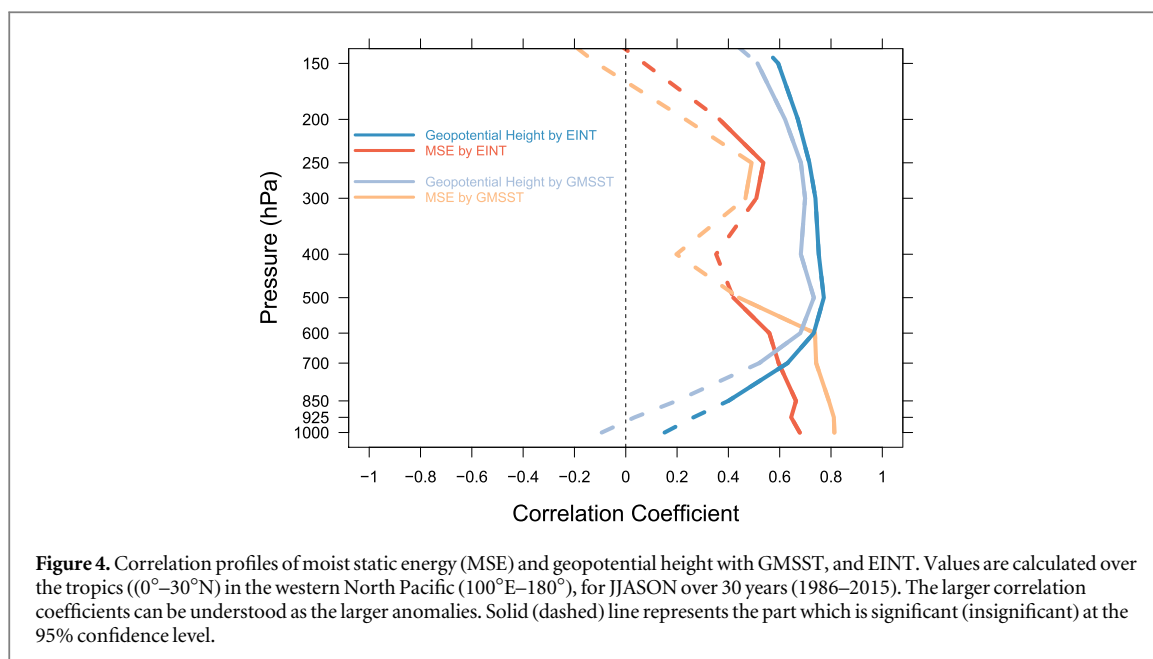
Table 2. The lower and upper limits of 95% interval of each variance partitions. Values come from the correlation coefficient between the two variables, and are rounded to the first digit after the decimal point.

	Lower limit	Estimate (%)	Upper limit
RIp and EINT	37.9	63.8	81.0
RIp and GMSST	23.0	51.3	73.2
RIp and negative SOI	0.2	16.1	44.3
RIp and ATg	12.8	40.5	65.7

gets larger when AT_{RI} decreases. AT is used for the scaling factor in the denominator in order to remove the variation of AT itself. Partitioning of the variance reveals that ATg explains 40.5% of the RIp variance. It is interpreted as the AT at the RI-experiencing LMIs are likely to be shorter than overall LMIs. It is also found that this quicker development for RI can be explained mostly (72.6%) by EINT.

EINT provides a physical explanation of how global warming influences RI. It is not only a statistical artifact. The physical process of global warming and its contribution to EINT has been argued in previous studies (Kang and Elsner 2015, Yang *et al* 2018), and Kang and Elsner (2016) presented the vertical structure by

the spatial pattern of anomalous high and SST in the region. Results showed that the more unstable atmosphere coupled with anomalous high pressure induced by global warming makes EINT more dominant than ever. Figure 4 compares the correlation profiles of MSE and geopotential height with GMSST, EINT, and RIp. The correlation coefficients of the two environmental factors including MSE and geopotential height with GMSST confirm that global warming favors an environment where these two factors act in opposite directions. It is noted that EINT contributes the largest variance to geopotential height while GMSST contributes the largest variance to MSE. In consideration of the larger portion of EINT than GMSST in RIp variance (see figure 3(a)), this anomalous high for EINT seems more effective to RIp than the MSE increase by GMSST. The EINT environment is identified as the atmospheric structure on the climate scale where fewer TCs occur but when they do they blast to release the available energy. The shorter AT (on average) to RI-experiencing LMIs relative to all LMIs (see figure 3(c)) also supports the blasting nature of the EINT environment. Along with the findings in figure 3, global warming is likely to form an EINT-like environment which provides favorable conditions for RI events. EINT environment also explains why the number of RI-experiencing LMIs is not increasing



over time since it is understood as the balance between the inhibition of TC genesis and increasing RIp, both by the EINT-like environment of global warming.

6. Summary and discussion

RI of TCs as a consequence of global warming is of increasing concern. This study examines how western North Pacific TC RI is related to the EINT environment induced by global warming. The EINT environment implies favorable conditions for the stronger intensity with fewer TCs (Kang and Elsner 2015). The study uses annual (JJASON) best-track data over a 30 year period (1986–2015). Results from the study can be summarized into the following three questions and their answers:

- (1) What is the global warming influence on western North Pacific TC RI?
 - Global warming significantly increases the proportion of RI-experiencing TCs. Global warming explains up to 51.3% of the variation in the proportion of RI-experiencing TCs with 93.0% of that related to EINT. EINT explains 63.8% of the variance of the proportion of RI-experiencing TCs, meaning EINT plays an important role in western North Pacific TC RI. The EINT environment is characterized by a strongly anomalous high pressure at middle and upper altitudes and an unstable tropical atmosphere, which is confirmed to accompany the quick process of TC intensification. Even the influence of ENSO on the proportion of RI events, though small, is mostly through an EINT environment. Shorter AT to LMIs of RI-experiencing TCs relative to the AT to LMIs of all TCs supports the nature of EINT.
- (2) Is the number of RI events increasing over time?
 - No. Despite the increasing proportion of RI events among TCs, the number shows no trend over time. Through the inhibition of overall TC genesis, EINT-like environment led by global warming is the reason for the unchanging number of RI events. As no trend is examined in ENSO (indicated by negative SOI) at least in the study period, its influence is not considered for interpretation.
- (3) How can the findings from different TC best-track sources reach an observational consensus?
 - Different wind averaging periods among the best-track sources such as JTWC and JMA have long been a problem. Based on an assumption that the rank probabilities of a certain intensity TC in two different best-track data would be the same (Kang and Elsner 2012b, 2016), this study first time finds a conversion fit of JMA LMIs to the values equivalent to JTWC observations. The consensus between the two 1 min LMI sets from JTWC and JMA are confirmed by the two-dimensional density distribution of LMI and AT at the LMI. In addition, a merged version of TC indicators is constructed with the in-phase mode of principal components using the two best-track data sets. Significant responses of the merged TC indicators to the environmental factors can be regarded as an observational consensus.

This study shows that the global warming influence on the number and proportion of western North Pacific TC RI events is mainly through EINT conditions. By doing so the study lends additional support

for the growing evidence that global warming influences TC intensity. The findings are expected to help further investigations that make use of individual environmental factors (e.g. vertical wind shear) accompanying the climate variabilities of ocean heat and ENSO.

Here, we suggest one thing to take into account for understanding the global warming influence on RI. The point is that the global warming indicated by annual GMSST may include the contribution of internal variabilities as well as other forcings. As Wang *et al* (2015) presented the similar results on RI features by investigating the relationship with the Pacific Decadal Oscillation (PDO), the internal variability is considered as sharing some part of the global warming influence, especially on relatively shorter timescales (Bjerknes 1966, Kang and Elsner 2018). For better understanding of the contribution by the internal variability, the variance portions of PDO and detrended-GMSST in detrended-RIp could be examined. The results show that 35.0% of detrended-RIp is explained by detrended-GMSST, and 63.1% of the detrended-GMSST contribution is made by PDO. Future investigations with longer observation data are expected to help with further discerning the contribution of forced global warming from the internal variabilities.

Acknowledgments

This work was supported by the National Typhoon Center at the Korea Meteorological Administration ('Research and Development for Numerical Weather Prediction and Earthquake Services in KMA').

ORCID iDs

Nam-Young Kang  <https://orcid.org/0000-0003-3018-9038>

References

- Bjerknes J 1966 A possible response of the atmospheric hadley circulation to equatorial anomalies of ocean temperature *Tellus* **18** 820–9
- Chu J H, Sampson C R, Levine A S and Fukada E 2002 *The Joint Typhoon Warning Center Tropical Cyclone Best-Tracks, 1945–2000 Rep. NRL/MR/7540-02-16* Joint Typhoon Warning Center
- Elsberry R L 2014 Advances in research and forecasting of tropical cyclones from 1963–2013 *Asia-Pac. J. Atmos. Sci.* **50** 3–16
- Elsberry R L, Lambert T D B and Boothe M A 2007 Accuracy of Atlantic and eastern North Pacific tropical cyclone intensity forecast guidance *Weather Forecast.* **22** 747–62
- Elsner J B, Kossin J P and Jagger T H 2008 The increasing intensity of the strongest tropical cyclones *Nature* **455** 92–5
- Emanuel K A 2017 Will global warming make hurricane forecasting more difficult? *Bull. Am. Meteorol. Soc.* **98** 495–501
- Gao S, Zhang W, Liu J, Lin I-I, Chiu L S and Cao K 2016 Improvements in typhoon intensity change classification by incorporating an ocean coupling potential intensity index into decision trees *Weather Forecast.* **31** 95–106
- Houser T *et al* 2015 *Economic Risks of Climate Change: An American Prospectus* (New York, USA: Columbia University Press) 9780231174565
- Huang B, Thorne P, Smith T, Liu W, Lawrimore J, Banzong V, Zhang H, Peterson T and Menne M 2015 Further exploring and quantifying uncertainties for extended reconstructed sea surface temperature (ERSST) version 4 (v4) *J. Clim.* **29** 3119–42
- Kang N-Y and Elsner J B 2012a An empirical framework for tropical cyclone climatology *Clim. Dyn.* **39** 669–80
- Kang N-Y and Elsner J B 2012b Consensus on climate trends in western North Pacific tropical cyclones *J. Clim.* **25** 7564–73
- Kang N-Y and Elsner J B 2015 Trade-off between intensity and frequency of global tropical cyclones *Nat. Clim. Change* **5** 661–4
- Kang N-Y and Elsner J B 2016 Climate mechanism for stronger typhoons in a warmer world *J. Clim.* **29** 1051–7
- Kang N-Y and Elsner J B 2018 The changing validity of tropical cyclone warnings under global warming *NPJ Clim. Atmos. Sci.* **1** 36
- Kaplan J and DeMaria M 2003 Large-scale characteristics of rapidly intensifying tropical cyclones in the North Atlantic basin *Weather Forecast.* **18** 1093–108
- Kaplan J, DeMaria M and Knaff J A 2010 A revised tropical cyclone rapid intensification index for the Atlantic and eastern North Pacific basins *Weather Forecast.* **25** 220–41
- Knapp K R and Kruk M C 2010 Quantifying interagency differences in tropical cyclone best-track wind speed estimates *Mon. Weather Rev.* **38** 1459–73
- Kowch R and Emanuel K 2015 Are special processes at work in the rapid intensification of tropical cyclones? *Mon. Weather Rev.* **143** 878–82
- Lee C-Y, Tippett M K, Sobel A H and Camargo S J 2016 Rapid intensification and the bimodal distribution of tropical cyclone intensity *Nat. Commun.* **7** 10625
- Lin I-I *et al* 2013 An ocean coupling potential intensity index for tropical cyclones *Geophys. Res. Lett.* **40** 1878–82
- Mendelsohn R, Emanuel K, Chonabayashi S and Bakkensen L 2012 The impact of climate change on global tropical cyclone damage *Nat. Clim. Change* **2** 205–9
- NDRRMC 2014, Updates re the effects of typhoon 'yolanda' (haiyan) (www.ndrrmc.gov.ph/attachments/article/1329/FINAL_REPORT_re_Effects_of_Typhoon_YOLANDA_HAIYAN_06-09NOV2013.pdf)
- Rappaport E N, Jiing J-G, Landsea C W, Murillo S T and Franklin J L 2012 The joint hurricane test bed: its first decade of tropical cyclone research-to-operations activities reviewed *Bull. Am. Meteorol. Soc.* **93** 371–80
- Rogers R F, Reasor P D and Lorsolo S 2013 Airborne Doppler observations of the inner-core structural differences between intensifying and steady-state tropical cyclones *Mon. Weather Rev.* **141** 2970–91
- Song J J, Wang J and Wu L 2010 Trend discrepancies among three best track data sets of western North Pacific tropical cyclones *J. Geophys. Res.* **115** D12128
- Velden C *et al* 2006 The Dvorak tropical cyclone intensity estimation technique: a satellite-based method that has endured for over 30 years *Bull. Am. Meteorol. Soc.* **87** 1195–210
- Wang B and Zhou X 2008 Climate variation and prediction of rapid intensification in tropical cyclones in the western North Pacific *Meteorol. Atmos. Phys.* **99** 1–16
- Wang C, Wang X, Weisberg R H and Black M L 2017 Variability of tropical cyclone rapid intensification in the North Atlantic and its relationship with climate variations *Clim. Dyn.* **49** 3627–45
- Wang X, Wang C, Zhang L and Wang X 2015 Multidecadal variability of tropical cyclone rapid intensification in the western North Pacific *J. Clim.* **28** 3806–20
- Yang S-H, Kang N-Y, Elsner J B and Chun Y 2018 Influence of global warming on western North Pacific tropical cyclone intensities during 2015 *J. Clim.* **31** 919–25